C-A/AP/21
December 2000

Update of the LHC Interaction Region Nonlinear Corrector Studies

W. Fischer, F. Pilat and V. Ptitsin

Collider-Accelerator Department
Brookhaven National Laboratory
Upton, NY 11973

BNL C-AD/AP/21

Update of the LHC Interaction Region Nonlinear Corrector Studies

W. Fischer, F. Pilat and V. Ptitsin

Abstract

The LHC interaction region nonlinear local correction system is studied with the latest error tables. Distributions of corrector strength are obtained from random field error distributions. Short- and long-term tracking is used to investigate whether a number of higher order correction layers can be omitted without performance degradation.

1 Introduction

In this report we provide an update of the studies aimed at evaluating the effectiveness of LHC interaction region nonlinear correction system. These studies have been performed in the frame of the US-LHC collaboration. One of the US contributions to the LHC project is the construction of the superconducting magnets (both dipole and quadrupoles) for LHC interaction regions and RF section. The interaction region triplet quadrupoles are constructed by FNAL and KEK (Japan) while the separation dipoles by BNL.

To compensate for unavoidable high harmonic magnet field errors in the magnets a set of correcting elements utilizing different harmonic corrector layers will be installed among the triplet quadrupoles. The studies presented here used the LHC collision lattice since it is at collision that the nonlinear errors from the IR magnets dominate the beam dynamics, given the large beta function in the interaction region quadrupoles.

2 Correction system

The schematics of LHC IR triplet correctors is shown in Fig. 1. The subject of our analysis is to determine the optimal number and settings for the high order corrector layers. The number of the corrector layers has to be sufficiently large to minimize the effect of the nonlinear field errors from interaction region quadrupoles and dipoles on the beam. Two schemes of nonlinear corrector layers were considered. Scheme 1 includes all normal and skew nonlinear corrector layers from order 3 (sextupole) to 6 (dodecapole). Scheme 2 omits the b_5, a_5 and a_6 corrector layers.

Two quantities are used to evaluate the effect of nonlinear field errors: tune footprints and dynamic aperture. The target values for the tune spread is less than 10^{-3} over 6σ. For the dynamic aperture, an average of at least 12σ and a minimum of at least 10σ are the target figures for 10^5 turns. The average and minimum are obtained over a reasonable number of seeds. We use 10 seeds in most cases.

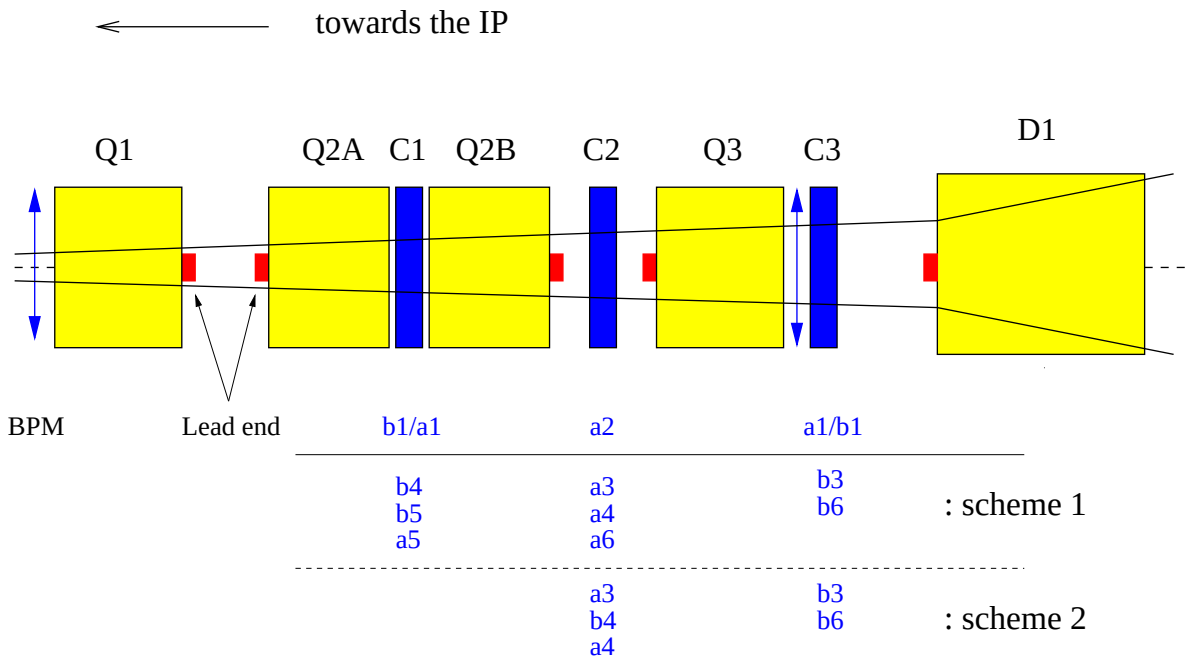

Figure 1: LHC interaction region corrector setup for two considered sets of nonlinear corrector layer arrangement. C1,C2,C3 are the corrector modules. b_1 corresponds to the normal dipole harmonic.

Most results presented in this report use the most recent versions of the expected field error tables, namely v4.0 for KEK quadrupoles and v3.1 for FNAL quadrupoles. The corrector strength analysis presented in Sec. 3 compares the data with early versions of the error tables. Some studies were also done with the KEK error table v4.x. In this version the KEK random errors are replaced by the FNAL random errors from v3.1. Results for earlier error tables can be found in references [1–5]. Error tables are given at Ref. [7].

The sum of mean and uncertainty of the magnetic errors in the error tables were interpreted as systematic errors in simulations. A distribution of random errors was created with 10 seeds using the rms values in the tables.

The corrector strengths are determined by using the action-angle kick minimization method [6]. In this method the change in the action variable induced by nonlinear field errors and nonlinear field correctors is minimized separately for each specified multipole field harmonic and for each interaction region.

3 Distributions of Corrector Strengths

Distributions of the nonlinear interaction region correctors at IP1 and IP5 were determined for the KEK v3.0 and FNAL v3.0 error tables. The distributions were created with 10 seeds for each sign of the systematic error part. With two correctors in each interaction

region, a total of 80 values for each multipole corrector type (b_3 to b_6 and a_3 to a_6) is generated.

In tables 1 and 2 these distributions are shown for each corrector layer. The first column shows distributions of all 80 seeds, the second column shows the distributions for a positive sign of the systematic errors, the third column shows the distributions for a negative sign of the systematic errors. The distributions of all 80 seeds have been fitted with the function

$$y = a \exp\left\{-b(x-c)^2\right\} \tag{1}$$

where x denotes the corrector strength (in units of 10^{-4}) and y the frequency of a given corrector strength. The central value c is read off the distribution charts and the values a and b are fitted. The fitted functions are shown in the first column in tables 1 and 2.

Except for b_6, all distributions show a maximum near zero corrector strength and rapidly decrease with increasing corrector strength. For b_6, an allowed harmonic of the main quadrupole field, the distribution has a non-zero maximum and a Gaussian distribution around it.

The strength distributions for b_5, a_5 and a_6 show that it is unlikely that more than a few units are needed for the local nonlinear correction of the field errors. This suggests that these correctors can be eliminated.

In Tab. 3 a summary of the corrector strength distributions for different error tables is shown for IP1 and IP5. In each and every case the necessary corrector strength is smaller than the available one.

In general there is a steady improvement following the evolution of the error tables. The errors of the warm D1 magnets with error table v1.0 have no significant effect on the corrector strength. KEK v4.x is a notion for an error distribution with systematic errors taken from KEK v4.0 and random errors from FNAL v3.1 . In this case the corrector strengths are significantly reduced compared to the KEK v4.0/FNAL v3.1 case.

In table 4 the corrector strength distributions are summarized for IP2, used in ion operation, and the analysis of this leads to the same conclusions as the analysis of table 3.

Table 1: Distributions of **normal** corrector strengths. Shown are the distributions of all tested seeds with and exponential fit, the distributions which have a positive sign in the systematic error part, and the distributions which have a negative sign in the systematic error part.

All seeds | **Systematic error positive** | **Systematic error negative**

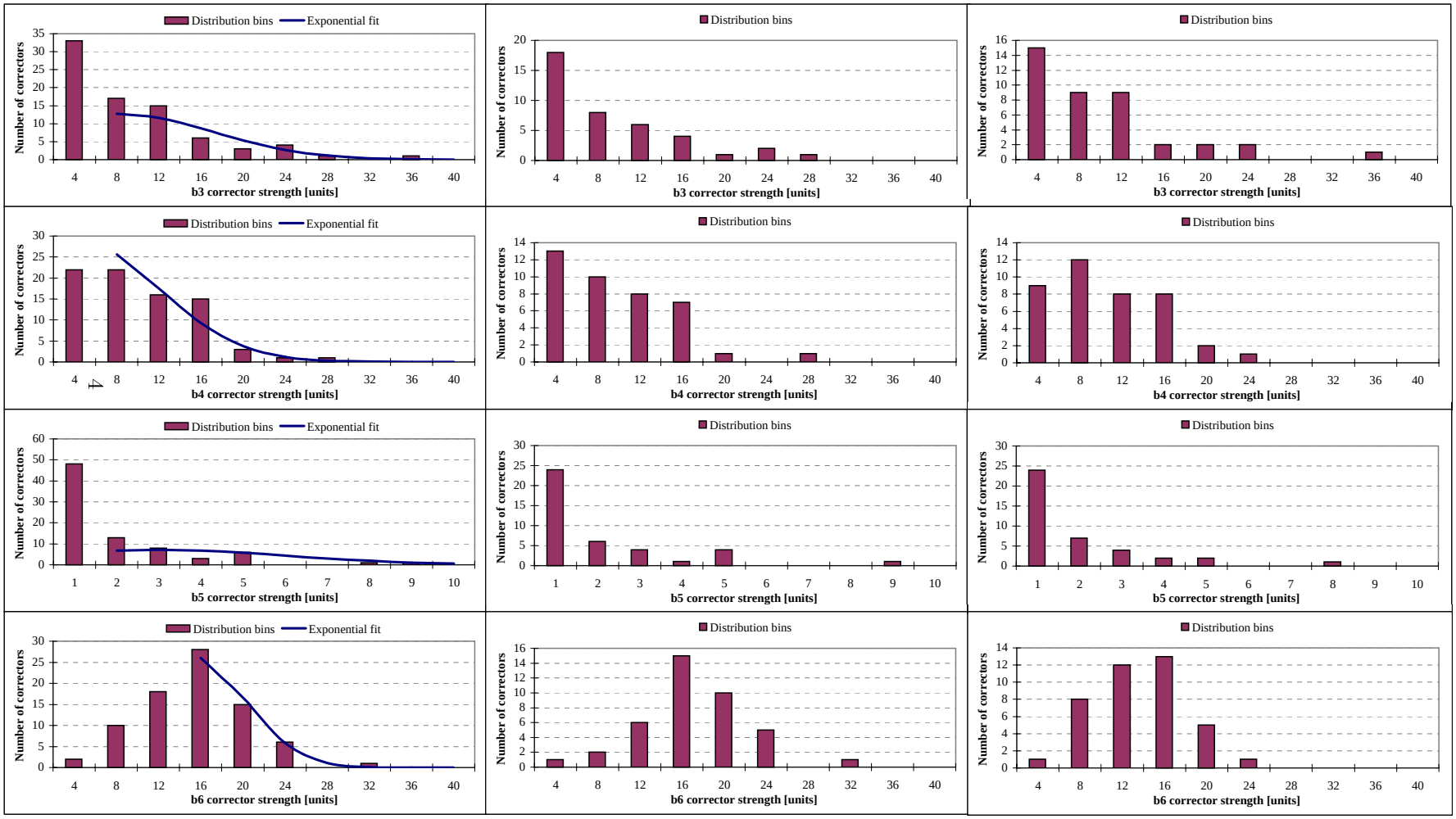

Table 2: Distributions of **skew** corrector strengths. Shown are the distributions of all tested seeds with and exponential fit, the distributions which have a positive sign in the systematic error part, and the distributions which have a negative sign in the systematic error part.

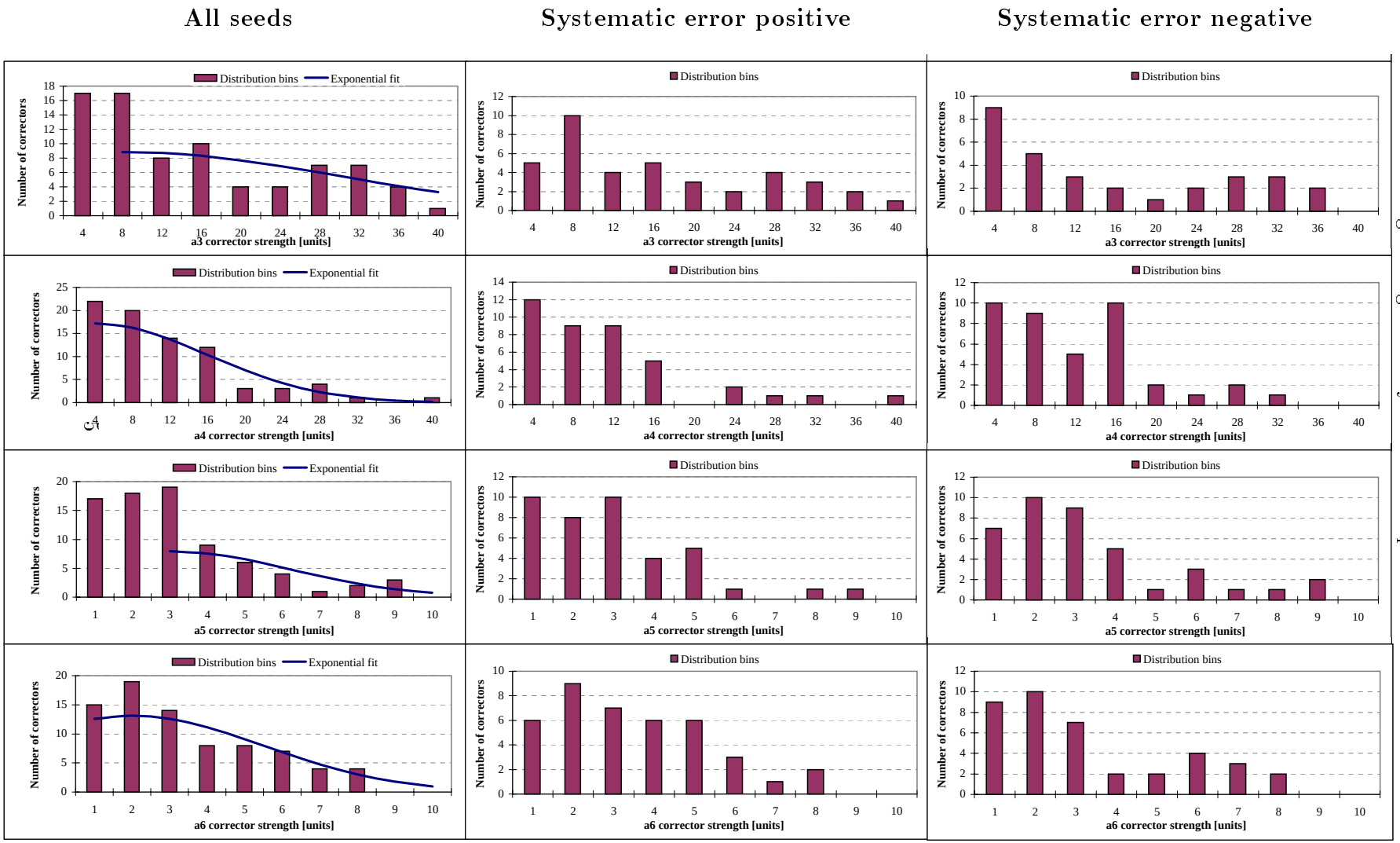

Table 3: Corrector strengths at **IP1** and **IP5** for different error tables.

Multipole European		KEK v2.0 FNAL v2.0 needed [Tesla]	KEK v3.0 FNAL v2.0 needed [Tesla]	KEK v3.0 FNAL v3.0 needed [Tesla]	KEK v3.0 FNAL v3.0 2xD1W v1.0 needed [Tesla]	KEK v4.0 FNAL v3.1 2xD1W v1.0 needed [Tesla]	KEK v4.x FNAL v3.1 2xD1W v1.0 needed [Tesla]	available [Tesla]
$\mathbf{b_3}$	mean	0.0023	0.0025	0.0025	0.0022	0.0028	0.0013	
	σ	0.0027	0.0026	0.0023	0.0018	0.0023	0.0011	
	mean+3σ	0.0104	0.0102	0.0094	0.0074	0.0098	0.0047	
	max	0.0120	0.0128	0.0110	0.0075	0.0097	0.0044	0.1000
$\mathbf{b_4}$	mean	0.0029	0.0039	0.0027	0.0027	0.0027	0.0026	
	σ	0.0021	0.0030	0.0019	0.0018	0.0017	0.0010	
	mean+3σ	0.0092	0.0128	0.0083	0.0082	0.0078	0.0057	
	max	0.0085	0.0133	0.0090	0.0067	0.0074	0.0054	0.0660
$\mathbf{b_5}$	mean	0.0009	0.0007	0.0004	0.0006	0.0004	0.0002	
	σ	0.0011	0.0009	0.0006	0.0007	0.0005	0.0003	
	mean+3σ	0.0042	0.0033	0.0022	0.0028	0.0017	0.0012	
	max	0.0033	0.0036	0.0028	0.0029	0.0018	0.0014	0.0370
$\mathbf{b_6}$	mean	0.0037	0.0050	0.0045	0.0045	0.0054	0.0053	
	σ	0.0021	0.0023	0.0017	0.0022	0.0021	0.0015	
	mean+3σ	0.0100	0.0118	0.0095	0.0110	0.0118	0.0099	
	max	0.0092	0.0119	0.0098	0.0098	0.0107	0.0084	0.0200
$\mathbf{a_3}$	mean	0.0055	0.0072	0.0047	0.0054	0.0049	0.0024	
	σ	0.0049	0.0055	0.0038	0.0038	0.0038	0.0017	
	mean+3σ	0.0202	0.0236	0.0162	0.0168	0.0163	0.0077	
	max	0.0194	0.0230	0.0138	0.0177	0.0151	0.0082	0.1550
$\mathbf{a_4}$	mean	0.0063	0.0036	0.0032	0.0034	0.0027	0.0020	
	σ	0.0041	0.0031	0.0027	0.0023	0.0020	0.0016	
	mean+3σ	0.0186	0.0128	0.0113	0.0103	0.0088	0.0067	
	max	0.0175	0.0158	0.0130	0.0086	0.0081	0.0072	0.0860
$\mathbf{a_5}$	mean	0.0016	0.0011	0.0009	0.0010	0.0006	0.0004	
	σ	0.0011	0.0008	0.0008	0.0007	0.0005	0.0003	
	mean+3σ	0.0050	0.0036	0.0033	0.0031	0.0021	0.0011	
	max	0.0047	0.0040	0.0040	0.0032	0.0019	0.0011	0.0440
$\mathbf{a_6}$	mean	0.0008	0.0010	0.0010	0.0009	0.0005	0.0003	
	σ	0.0006	0.0008	0.0008	0.0007	0.0004	0.0002	
	mean+3σ	0.0027	0.0033	0.0033	0.0029	0.0018	0.0009	
	max	0.0024	0.0038	0.0036	0.0029	0.0022	0.0009	0.0200

Note 1: Strength is given as magnetic field at $R = 17$mm.
Note 2: Statistics with 80 values (10 seeds, 4 correctors, systematic errors with positive and negative sign). Note 3: KEK v4.x is KEK v4.0 with the FNAL v3.1 random errors.

Table 4: Corrector strengths at **IP2** for different error tables.

Multipole European		KEK v2.0 FNAL v2.0 needed [Tesla]	KEK v3.0 FNAL v2.0 needed [Tesla]	KEK v3.0 FNAL v3.0 needed [Tesla]	KEK v4.0 FNAL v3.1 needed [Tesla]	KEK v4.x FNAL v3.1 needed [Tesla]	available [Tesla]
$\mathbf{b_3}$	mean	0.0029	0.0037	0.0048	0.0055	0.0055	
	σ	0.0037	0.0036	0.0042	0.0043	0.0040	
	mean+3σ	0.0141	0.0144	0.0174	0.0183	0.0175	
	max	0.0115	0.0116	0.0195	0.0172	0.0154	0.1000
$\mathbf{b_4}$	mean	0.0031	0.0037	0.0032	0.0031	0.0029	
	σ	0.0022	0.0023	0.0025	0.0022	0.0015	
	mean+3σ	0.0097	0.0105	0.0107	0.0096	0.0073	
	max	0.0093	0.0088	0.0098	0.0077	0.0058	0.0660
$\mathbf{b_5}$	mean	0.0011	0.0011	0.0008	0.0007	0.0006	
	σ	0.0016	0.0017	0.0011	0.0009	0.0008	
	mean+3σ	0.0060	0.0061	0.0040	0.0035	0.0029	
	max	0.0060	0.0061	0.0041	0.0031	0.0025	0.0370
$\mathbf{b_6}$	mean	0.0055	0.0060	0.0041	0.0046	0.0043	
	σ	0.0015	0.0022	0.0016	0.0017	0.0011	
	mean+3σ	0.0101	0.0125	0.0088	0.0096	0.0076	
	max	0.0084	0.0099	0.0069	0.0071	0.0062	0.0200
$\mathbf{a_3}$	mean	0.0130	0.0126	0.0103	0.0116	0.0105	
	σ	0.0068	0.0072	0.0060	0.0049	0.0030	
	mean+3σ	0.0334	0.0342	0.0282	0.0262	0.0195	
	max	0.0228	0.0228	0.0218	0.0215	0.0162	0.1550
$\mathbf{a_4}$	mean	0.0080	0.0101	0.0066	0.0033	0.0034	
	σ	0.0060	0.0080	0.0059	0.0030	0.0025	
	mean+3σ	0.0259	0.0342	0.0243	0.0122	0.0110	
	max	0.0196	0.0248	0.0226	0.0121	0.0098	0.0860
$\mathbf{a_5}$	mean	0.0011	0.0011	0.0010	0.0005	0.0003	
	σ	0.0009	0.0009	0.0006	0.0004	0.0002	
	mean+3σ	0.0038	0.0038	0.0028	0.0016	0.0009	
	max	0.0030	0.0030	0.0020	0.0012	0.0009	0.0440
$\mathbf{a_6}$	mean	0.0015	0.0014	0.0014	0.0011	0.0010	
	σ	0.0010	0.0011	0.0010	0.0006	0.0005	
	mean+3σ	0.0045	0.0047	0.0042	0.0030	0.0024	
	max	0.0038	0.0041	0.0043	0.0025	0.0019	0.0200

Note 1: Strength is given as magnetic field at $R = 17$mm.
Note 2: Statistics for KEK v2.0/FNAL v2.0 and KEK v3.0/FNAL v2.0 with 20 values (10 seeds, 2 correctors), all other cases with 40 values (10 seeds, 2 correctors, systematic errors with positive and negative sign).

4 Tracking Results

We used TEAPOT for the tracking studies. As described in Sec. 2, ten seeds of magnet errors were created based on the expected error tables for the interaction region quadrupoles and dipoles. Five ratios of horizontal to total transverse emittance (sum of horizontal and vertical) were investigated. For each ratio initial conditions are taken at increasing amplitudes. For dynamic aperture tracking, synchrotron motion was included (using a total gap voltage of 16 MV). Tracking for tune footprints disregarded synchrotron motion.

To obtain the most conservative estimates for tune footprints and dynamic aperture, the LHC lattice for ion operation was chosen for tracking. In this case, the machine is configured with three low-beta insertions at IP1, IP2 and IP5, where $\beta_x^* = \beta_y^* = 0.5$. The nominal crossing angle of ± 150 μrad was used at all low-beta interaction points.

Tab. 5 and Figs. 2-4 summarize the results of the 1000-turn tracking studies. The horizontal axis in this plot shows the ratio of horizontal to total transverse emittance; 0 corresponds to the vertical, 1 to the vertical direction. The results can be summarized as follows:

1. Without nonlinear correctors, even the short-term dynamic aperture (1000 turns) is below the target values: 12σ average and 10σ minimum.
2. Applying all correctors (scheme 1 in Fig. 1) increases the dynamic aperture by about 4σ and puts it well above the target values.
3. Turning off the b_5, a_5 and a_6 correctors (scheme 2 in Fig. 1) decreases the dynamic aperture by about 0.5σ compared to the full corrector set. The 1000-turn dynamic aperture is still well above the target values.

Table 5: Summary of 1000 turn tracking runs. The dynamic aperture (DA) is quoted in units of transverse rms size.

	Average DA	DA rms	Minimum DA
FNAL3.1,KEK4.0; correctors off	10.6	2.0	7
FNAL3.1,KEK4.x; correctors off	11.7	1.2	10
FNAL3.1,KEK4.0; all correctors on	15.2	2.2	12
FNAL3.1,KEK4.x; all correctors on	15.5	1.7	13
FNAL3.1,KEK4.0; b_5, a_5, a_6 off	14.9	2.2	11

The configuration with the reduced corrector set (without b_5, a_5, a_6) was further investigated with tracking over 10^5 turns. Fig. 5 shows the results of the long-term tracking. The average dynamic aperture is 13.7σ while the minimum dynamic aperture is 11σ, both above the target values.

The typical tune footprints obtained from the tracking are shown in Fig. 6. Without the correctors the tune spread for the particles with 6σ amplitude is a few units of 10^{-3}. With the triplet correctors on the tune footprints are contracted to less than 10^{-3}, thus fulfilling the target value.

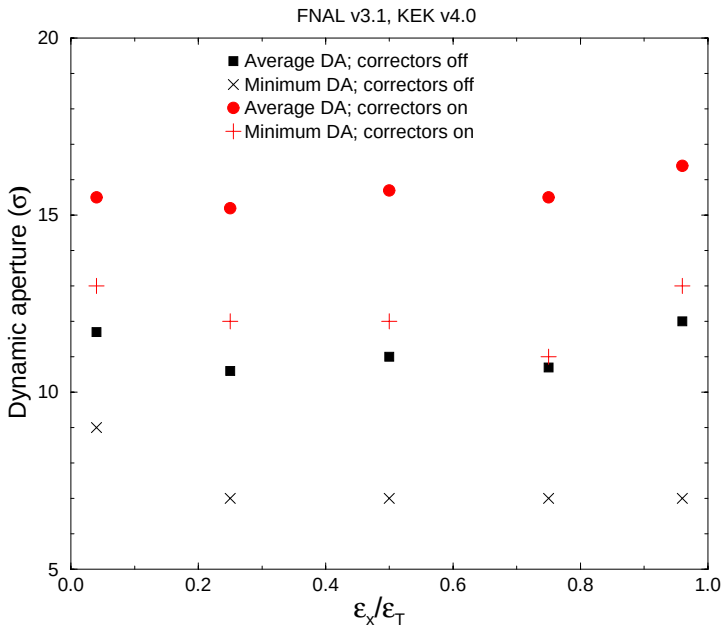

Figure 2: Dynamic aperture from 1000 turn tracking for the error table versions 3.1(FNAL) and 4.0(KEK).

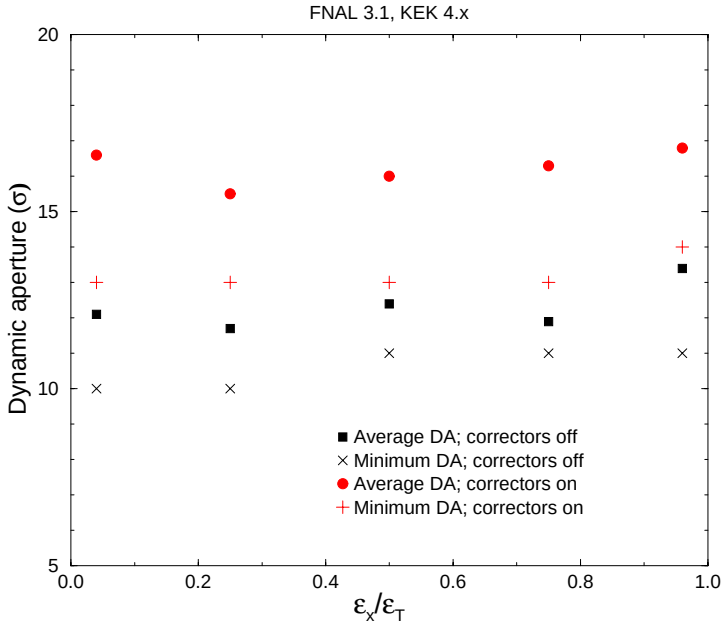

Figure 3: Dynamic aperture from 1000 turn tracking for the error table versions 3.1(FNAL) and 4.x(KEK).

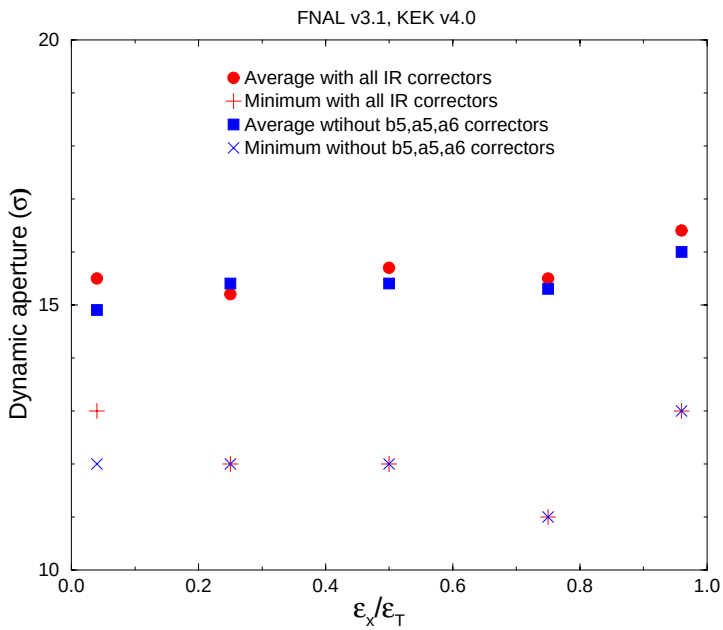

Figure 4: , The comparison of dynamic aperture from 1000 turn tracking for the error table versions 3.1(FNAL) and 4.0(KEK) obtained with whole corrector set and with a set that does not include b_5, a_5, a_6 corrector layers.

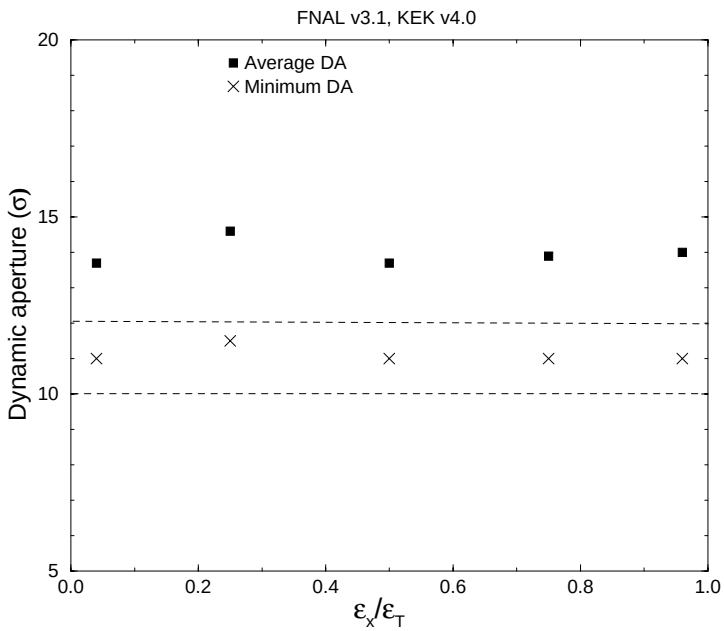

Figure 5: Dynamic aperture from 100000 turn tracking for the error table versions 3.1(FNAL) and 4.0(KEK). The reduced corrector set is used (without b_5, a_5, a_6 corrector layers).

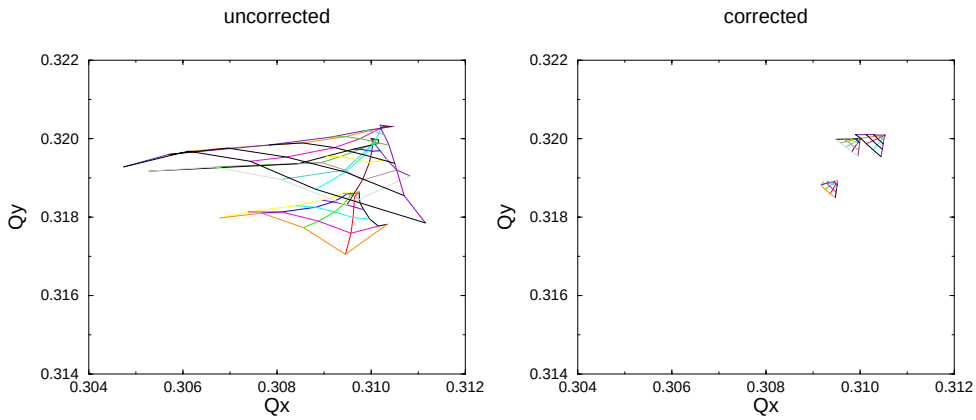

Figure 6: 6σ tune footprints with the triplet correctors off and on. The three tune footprints correspond to $\Delta p/p = 0; \pm 0.28 \cdot 10^{-3}$

5 Conclusion

The LHC interaction region nonlinear corrector system shown in Fig. 1 is adequate to compensate for the expected high order field errors in the interaction region magnets. The corrector layers for the b_5, a_5 and a_6 harmonics can be omitted with only minimal performance degradation.

References

[1] W. Fischer, V. Ptitsin, J. Wei, R. Ostojic and J. Strait, "LHC Interaction Region Correction Scheme Studies", proceedings of the Workshop on LHC Interaction Region Correction Systems, Upton, New York, BNL-52575 Formal Report, LHC Project Note 199 (1999).

[2] T. Sen, N. Gelfand and W. Wan, "Correction Schemes for the LHC Lattice at Collision", proceedings of the Workshop on LHC Interaction Region Correction Systems, Upton, New York, BNL-52575 Formal Report, LHC Project Note 199 (1999).

[3] V. Ptitsin, W. Fischer, J. Wei, "LHC Interaction Region Correction in Heavy Ion Operation", proceedings of the Workshop on LHC Interaction Region Correction Systems, Upton, New York, BNL-52575 Formal Report, LHC Project Note 199 (1999).

[4] V. Ptitsin, S. Tepikian, J. Wei, "BNL-Built LHC Magnet Error Impact Analysis and Compensation", proceedings of the 1999 Particle Accelerator Conference, New York (1999).

[5] J. Wei, W. Fischer, V. Ptitsin, R. Ostojic and J. Strait, "Interaction Region Local Correction for the Large Hadron Collider" proceedings of the 1999 Particle Accelerator Conference, New York (1999).

[6] J. Wei, "Principle of Interaction Region Correction", proceedings of the Workshop on LHC Interaction Region Correction Systems, BNL-52575 Formal Report, LHC Project Note 199.

[7] http://www.rhichome.bnl.gov/LHC/ref